DOI 10.1007/978-1-4899-7413-6_17
Reprinted from *Space Science Reviews* Journal, DOI 10.1007/s11214-013-9969-6

Microphysics of Quasi-parallel Shocks in Collisionless Plasmas

D. Burgess · M. Scholer

Received: 17 October 2012 / Accepted: 13 February 2013 / Published online: 1 March 2013

Abstract Shocks in collisionless plasmas require dissipation mechanisms which couple fields and particles at scales much less than the conventional collisional mean free path. For quasi-parallel geometries, where the upstream magnetic field makes a small angle to the shock normal direction, wave-particle coupling produces a broad transition zone with large amplitude, nonlinear magnetic pulsations playing an important role. At high Mach numbers, ion reflection and acceleration are dominant processes which control the structure and dissipation at the shock. Accelerated particles produce a precursor, or foreshock, characterized by low frequency magnetic waves which are convected by the plasma flow into the shock transition zone. The interplay between energetic particles, waves, ion reflection and acceleration leads to a complicated interdependent system. This review discusses the spacecraft observations which have motivated the current view of the high Mach number quasi-parallel shock, and the theories and simulation studies which have led to a better understanding of the microphysics on which the quasi-parallel shock depends.

Keywords Space plasma · Collisionless shock · Particle acceleration

1 Introduction

Shocks in collisionless plasmas require dissipation mechanisms which couple fields and particles at scales much less than the conventional collisional mean free path. They cannot be understood without a study of the processes which operate and the resulting scale lengths and structure—in other words, the microphysics of the shock. Collisionless shocks are not only of interest in themselves, but also for the key role they play in universal mechanisms in cosmic plasmas such as particle acceleration and flow-obstacle interactions. The structure

D. Burgess (✉)
Astronomy Unit, Queen Mary University of London, London E1 4NS, UK
e-mail: D.Burgess@qmul.ac.uk

M. Scholer
Max-Planck-Institut für extraterrestrische Physik, 85740 Garching, Germany

and dissipation mechanisms affect the injection of particles into acceleration processes and thus are important for the overall acceleration efficiency. They are also vital for understanding how the shock behaviour and resulting particle acceleration may depend on the plasma environment and shock parameters. A companion review describes particle acceleration at the terrestrial bow shock (Burgess et al. 2012), and the mechanisms described therein can mostly be generalized to other regimes.

In a collisionless plasma a shock is primarily characterized by the shock strength or Mach number M, and magnetic geometry. The latter can be defined by the angle θ_{Bn} between the upstream magnetic field and the shock normal: if $\theta_{Bn} > 45°$ the shock is described as quasi-perpendicular, and otherwise quasi-parallel. For sufficiently high Mach number fluid models with only resistive dissipation are inconsistent, i.e., no stable solution can be found. For such shocks it is found in observations and simulations that they are dominated by ion dissipation deriving from reflection (usually near specular reflection) of some fraction of the incident distribution at the shock ramp. Ion reflection at the quasi-perpendicular shock changes the structure of the shock, both on average and in terms of the fluctuations generated at the shock. Such shocks are usually termed super-critical, where the critical Mach number is that above which no resistive fluid solutions can be found. We will see shortly that the sub/super-critical distinction is less applicable to the quasi-parallel shock due to the lack of a single, monotonic shock ramp corresponding to that found in low Mach number fluid solutions. However, as discussed in this review, at high Mach number ion reflection appears to play a crucial role for dissipation processes also within the quasi-parallel shock.

At the quasi-perpendicular shock the reflected ions gain perpendicular energy and their subsequent gyration and motion downstream produces strong ion heating. The upstream magnetic geometry and the particle gyration ensures that they remain within a gyro-scale of the shock ramp, and the average profiles for the magnetic field and other plasma quantities have some similarity to the laminar solutions of fluid models. There may be considerable contributions from fluctuations and internal structure at shorter scales, but the overall scale is set by the particle gyration of reflected ions. However, as θ_{Bn} is decreased the magnetic geometry dictates that the particle parallel velocity obtained via reflection may, if large enough, allow the particle to move away upstream from where it was reflected. Similarly, considering an energetic ion, or heated ion downstream but just at the shock ramp, it may have enough parallel velocity to escape upstream of the shock. In either case, it is clear that energetic, shock associated upstream particles are an intrinsic feature of the high Mach number quasi-parallel shock, and this is borne out by observations at the terrestrial bow shock and other heliospheric shocks. Upstream suprathermal particles can drive waves via plasma instabilities, and which in turn controls the diffusion properties of the energetic particles in the upstream region. In this way the foreshock (that region of space ahead of the shock filled with waves and particles by virtue of the shock itself) plays a central role in diffusive shock acceleration theory. The presence of energetic particles in the foreshock complicates the question of the dominant scale lengths at the quasi-parallel shock. We have seen that the gyro-scale is a characteristic scale at the quasi-perpendicular shock. But at the quasi-parallel shock the characteristic length scales depend on the coupling between waves and energetic particles, which in turn depends on the mechanisms for extracting energetic particles from the thermal distribution.

Early ideas, such as the work of Golden et al. (1973) and others, addressed the problem of how to link the upstream state (cold, high velocity) with that downstream (heated, slowed) by postulating an extended transition which was modelled as a gradual overlap between upstream and downstream states. The underlying assumption was that the transition had some degree of monotonicity in terms of average properties. This upstream/downstream

overlap is analogous to the idea that there was an "evaporation" of the heated downstream ions into an upstream precursor region, where they would produce a distribution function with parallel anisotropy unstable to the firehose instability (Parker 1961). The subsequent waves and relaxation would lead to the heating of ions as they passed through the precursor. Although conceptually attractive, these models, which relied on the idea of turbulent coupling, did not take into account many of the features of turbulence which are now believed to be important, such as the role of nonlinear interactions, intermittency, localized structures, etc. Parker's 1961 quote, however, seems prescient: "The relative importance of the precursor ... can be determined eventually by experiment or by sufficiently detailed machine calculations."

In terms of observations, these models, although important for introducing the idea of an extended coupling zone between upstream and downstream states, were dealt a blow by the early observations of the quasi-parallel terrestrial bow shock. Spacecraft observations will be discussed from a modern point of view in the next section. But it is instructive to consider the summary of Greenstadt et al. (1977) based on single spacecraft data, using instruments of only modest capability. They noted that the high Mach number quasi-parallel shock was characterized by "(1) Irregular large amplitude magnetic pulsations, sometimes in bursts, often separated by intervals of smaller amplitude upstream-like waves; (2) Thickness of $<2R_E$; (3) Large amplitude quasi-period transverse magnetic wave components; (4) Solar wind of nominally unreduced but significantly deflected streaming velocity; (5) Solar wind of elevated temperature, enhanced density, and distinct distribution with skewed high energy tails and irregular low-energy envelopes; ... (8) Interpulsation regions of upstream magnetic magnitude and wave structure but noisy, deflected, and partially thermalized plasma flow; (9) No direct evidence that the macrostructure was governed by fire hose instability as a dissipation mechanism." All these points survive in our current picture of the high Mach number quasi-parallel "pulsation" shock.

2 The Quasi-Parallel Pulsation Shock: Observations

Unlike traversals of the quasi-perpendicular bow shock, the terrestrial quasi-parallel shock often resembles a "hash" of multiple short-lived apparent transitions from upstream to downstream states, for example as in Fig. 1. Closer inspection shows a more complex structure, with variations of field, plasma speed and distribution function type. The quasi-parallel shock is associated with the ULF foreshock sited ahead of the shock and populated with energetic particles and ULF waves (see reviews in Burgess et al. 2005, 2012; Eastwood et al. 2005). One puzzling feature is that the amplitudes of structures seen in the quasi-parallel shock zone often exceed the downstream value that would be predicted from the shock jump (Rankine-Hugoniot) relations. This points to a lack of time-steady behaviour at the shock. A key breakthrough in the study of the terrestrial quasi-parallel bow shock was the dual spacecraft ISEE observations of Thomsen et al. (1990a) which showed that some of the magnetic pulsations within the shock transition had a "convective" signature. Typically the spacecraft velocity relative to the average bow shock position is small, of order a few km/s. Observations of the quasi-perpendicular shock occur when the bow shock position shifts and the shock moves across the spacecraft, either outwards or inwards. In contrast, when data from at least two spacecraft are combined, a convective signature in the relative timing of a feature in the time series indicates that the magnetic field structure is convecting with, or in the direction of the plasma. Magnetic pulsations in the quasi-parallel shock have a peak magnetic field amplitude which is at least, and often exceeds the average downstream

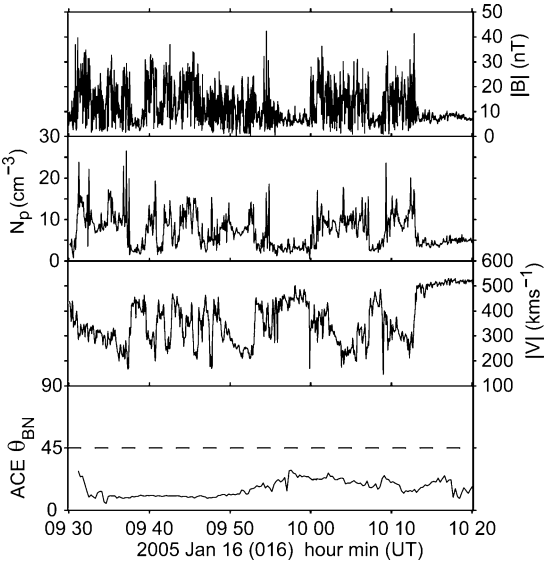

Fig. 1 Data from Cluster for a quasi-parallel shock crossing. Shown are magnetic field magnitude $|B|$ in nT, proton number density N_p in cm^{-3}, and plasma flow speed $|V|$ in km s^{-1}, all from Cluster 1. The *bottom panel* shows the angle θ_{Bn} estimated from upstream ACE data. From Lucek et al. (2008)

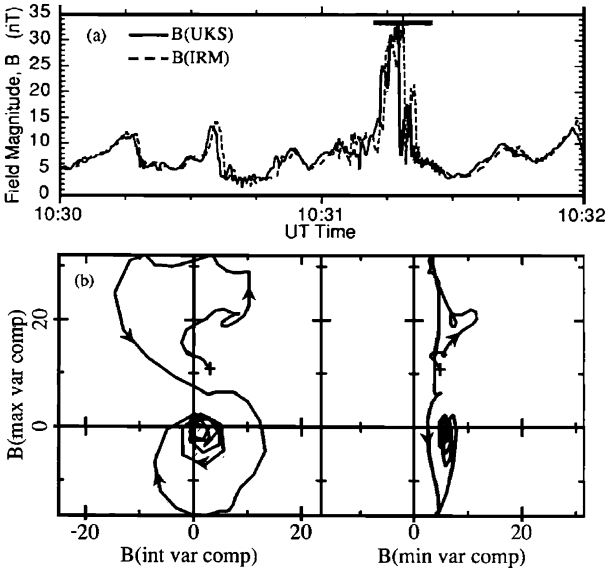

Fig. 2 Magnetic pulsation in data from AMPTE UKS and IRM, with (*below*) hodogram in minimum variance frame for the interval marked with a bar. From Schwartz et al. (1992)

value. The presence of a convective signature for some events therefore shows that these large values are achieved in magnetic field structures convecting in the flow, not merely by oscillations of a shock surface, as at the quasi-perpendicular shock.

Schwartz et al. (1992) distinguished between "isolated" pulsation events, with typical upstream solar wind on both sides, and "embedded" events which had a more complex form, with magnetosheath or partially heated solar wind on one or both sides. The isolated events have a well-defined monolithic appearance, lasting 5–20 s, a large peak magnetic field amplitude at least twice, but sometimes up to 5–6 times the solar wind value. Figure 2 shows a magnetic pulsation in data from AMPTE IRM and UKS. The relative timings are con-

sistent with convection in the direction of, but with a speed less than the solar wind. The hodogram shows that the initial part is LH polarized (in the spacecraft frame), the latter part RH polarized and in addition there is a LH polarized wave train consistent with a convected whistler. Different combinations of LH and RH polarization can be found at different pulsations, although the intrinsically RH polarized wave train, when seen, corresponds to a standing structure on the steepened upstream edge. For a convected pulsation this is seen as a standing structure on the trailing edge as observed in time. Similar structures are seen at the steepened edges of "shocklets" seen in the ULF wave foreshock, albeit at smaller amplitudes. Timing analysis indicates that the pulsations are typically propagating super-Alfvénically in the plasma rest frame, but slower than the solar wind speed, so that they are convected with the solar wind. The pulsation propagation speed increases with the peak amplitude of the magnetic field strength. Mann et al. (1994) found speeds between 2–5 v_A, which implies that the trailing (in time, i.e., upstream in space) edges of the larger pulsations are shock-like.

The complex magnetic structure of the quasi-parallel pulsation shock is reflected in the observations of ion particle distribution functions. It should be remembered that throughout the quasi-parallel shock and connected foreshock there is a population of energetic "diffuse" ions. However, at lower supra-thermal energies the ion distributions are highly variable with clumps of particles in velocity space. Gosling et al. (1989) reported evidence of (1) cold, coherent ion beams with velocities roughly consistent with specular reflection at a sharp gradient, and (2) downstream ion distributions which indicated the presence of a cold, deflected core, and a hotter low density shell in velocity space. They pointed out that similar features were seen at the quasi-perpendicular shock, implying that ion specular reflection could contribute, in the same manner, to ion dissipation at the quasi-parallel shock. However, this cannot be the complete picture since the observation of such distributions is intermittent, and the idea of a single shock surface acting to specularly reflect ions has to be reconciled with the behaviour of convecting pulsations which would disrupt that surface. Thomsen et al. (1990b) studied the ion distributions (in 2-D velocity space) downstream and presented evidence of two types of distribution: one with a cooler, denser core plus hot shell, and the other being a less dense, broader and more "Maxwellian" in appearance. These distributions would be observed in alternation close to the nominal shock transition. Thomsen et al. (1990b) argued that these two types of distribution were not evolutionary because the distribution far downstream had properties intermediate between the two initial states, and that examples of both types of distribution could be found at crossings of the shock ramp. Many of these results are refinements of the early Heos and Ogo observations presented in Greenstadt et al. (1977). Onsager et al. (1990), again using the ISEE 2-D ion experiment, performed a survey of coherent ion reflection in quasi-parallel shocks and found that such beams were detected frequently throughout the shock transition, and were seen near the shock ramp (identified in the electron density) or near other shock-like features (presumably pulsations). On the other hand, there are some shock-like features (pulsations) which are not seen associated with coherent ion beams. When cold coherent beams were observed they were almost always consistent with specular reflection after only a small fraction of a gyro-period after reflection. The observations of Onsager et al. (1990) and Thomsen et al. (1990b) indicate that ion specular reflection is important at some shock crossings, but not all. Or, more plausibly, time variability is crucial in interpreting any particular crossing. Another issue to be considered is the relatively low time resolution of particle instruments compared to magnetic field variations near pulsations, so that time-aliasing of observations is a real possibility.

The Onsager et al. (1990) observation that the specularly reflected ions are only seen as a coherent clump in velocity space shortly after reflection indicates that the ions are scattered,

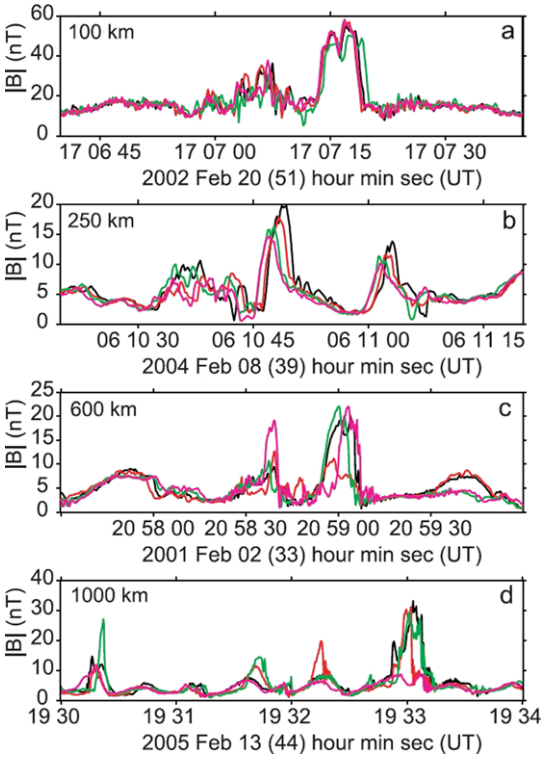

Fig. 3 Four examples of Cluster four spacecraft data for magnetic pulsations within the quasi-parallel shock transition. In each plot the *different colours* of the time series represent different spacecraft in the Cluster constellation. The approximate tetrahedron scale in km is marked for each case. From Lucek et al. (2008)

or coupled in some way to the rest of the plasma, relatively rapidly. It might be thought that the pulsations would be the source of that coupling, but another possibility is indicated by the observation that the dense, short-lived ion beams are associated with bursts of broad-band magnetic turbulence with frequencies up to at least 3 Hz, and possibly higher (Wilkinson et al. 1993). The magnetic turbulence was observed to be decorrelated between spacecraft at a separation of 150 km, making it difficult to fully analyse its properties. It was also found, with data from a 3D ion instrument, that cold ion beams could sometimes be seen which were inconsistent with specular reflection at the nominal shock orientation.

From the earliest studies it was acknowledged that single spacecraft observations cannot be used to distinguish the inherent propagation properties of fluctuations and pulsations, given the overall motion of the average bow shock. Multi-spacecraft observations give the possibility of establishing orientations of plasma structures, but only if there is sufficient time stability so that cross-correlation gives meaningful delay times between the spatially dispersed spacecraft. If there is considerable temporal evolution of a structure in the time that it convects past the spacecraft constellation, then it becomes impossible to determine orientations, and only some minimal information about scale lengths can be extracted. Cluster observations taken when the four spacecraft constellation had different separation scales are shown in Fig. 3 (Lucek et al. 2008). Different colours of the time series represent different spacecraft in the Cluster constellation. At a separation of 100 km (of order the ion inertial length) the time difference is less than one second, so that differences are more likely to be due to spatial gradients rather than temporal evolution. At separations of 250 km there is evidence of temporal evolution, and growth of the pulsation as it convects. Since the time difference is only of the order of a few seconds the growth is rapid, much less than

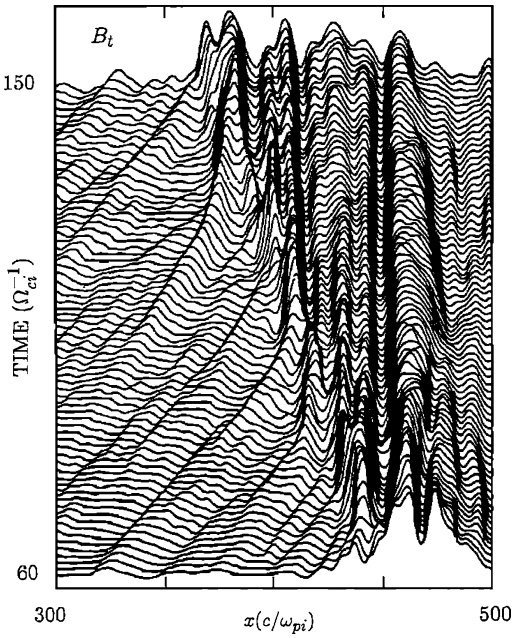

Fig. 4 Results from a hybrid simulation of a $\theta_{Bn} = 20°$, $M_A = 3.5$ shock. Shown are profiles of the magnetic field tangential to the shock stacked in time. From Scholer and Terasawa (1990)

the ion gyroperiod in the upstream magnetic field. For a separation of 600 km or 1000 km there are now considerable differences between the spacecraft profiles, and it is only possible to deduce the rather weak conclusion that temporal evolution and/or spatial gradients are important at those scales.

3 Simulations, Mechanisms and Microphysics

Hybrid simulations of quasi-parallel shocks above a Mach number of $M_A \sim 2$ have revealed that such shocks have a quasi-periodic cyclic behaviour in their structure, in that the abrupt transition of the magnetic field at the shock relaxes to a more gradual transition and is replaced by a new shock front ahead of the previous nominal shock position (Burgess 1989). Figure 4 (Scholer and Terasawa 1990) shows the time evolution of the transverse magnetic field component for a $\theta_{Bn} = 20°$, $M_A = 3.5$ shock as obtained from a 1-D hybrid simulation. The shock is launched off the right hand rigid wall of the simulation box, so that the shock propagates leftwards. From the left hand side upstream waves can be seen to run into the shock. These upstream waves are compressed closer to the shock; simultaneously the shock profiles becomes more gradual. The arriving wave steepens up at the upstream edge which becomes the newly reformed shock. Some of the reformation cycles are particularly prominent while others seem to be more like mini-cycles. On average reformation takes place every $20\Omega_c^{-1}$, corresponding to ~20 sec at Earth's bow shock.

The temporal development of the local shock normal angle and the occurrence of periodic bursts of backstreaming ions connected with the reformation process can be seen from Fig. 5 (Burgess 1995). These results are from a quasi-parallel 1-D hybrid shock simulation with $\theta_{Bn} = 30°$, $M_A = 6.5$, showing time evolution in the form of a grey scale plots of the total magnetic field B, the backstreaming ion density, and local instantaneous shock normal angle θ_{Bn}. The frame for the plots corresponds to the average shock rest frame. In all plots,

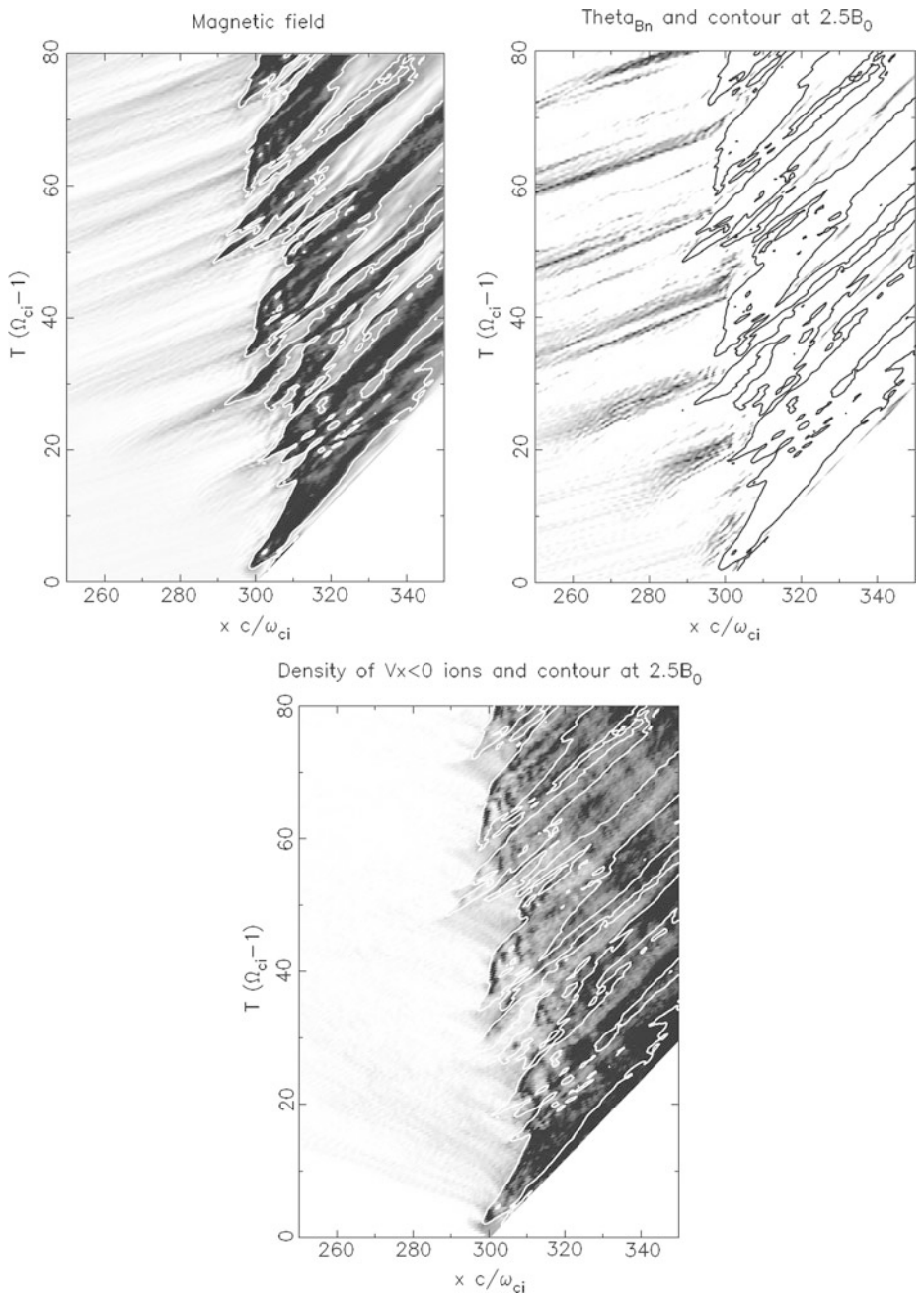

Fig. 5 Results from a quasi-parallel ($\theta_{Bn} = 30°$, $M_A = 6.5$) hybrid shock simulation showing time evolution in the shock frame of magnetic field (*white-black*: $0.9B_0 \rightarrow 3.5B_0$, with contour at $2.5B_0$), local instantaneous value of shock normal angle θ_{Bn} (*white-black*: $30° \rightarrow 5°$), and backstreaming ion density (*white-black*: $0.02 \rightarrow 2.0$). From Burgess (1995)

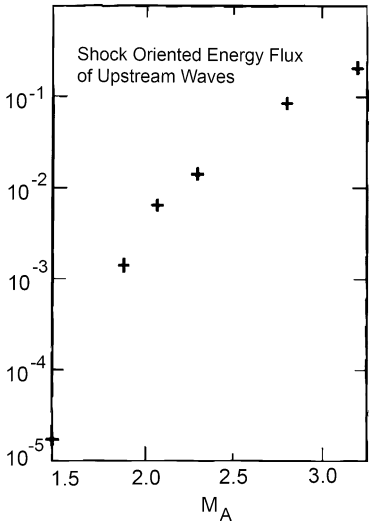

Fig. 6 Magnetic energy flux of upstream waves with downstream directed group velocity for 5 shocks with different Mach number ($\theta_{Bn} = 30°$). Adapted from Krauss-Varban and Omidi (1991)

a contour indicates where the total field is 2.5 times above its nominal upstream value, and thus the location of the main field jump. A major reformation cycle can be identified between $T = 42\Omega^{-1}$ and $T = 54\Omega^{-1}$, where the initial "shock" (i.e., location of an abrupt transition) moves backwards, and is replaced by another "shock" front ahead of the nominal shock position. This representation also reveals that there are mini-reformation cycles (e.g., at $T = 62\Omega^{-1}$), which some stack plot representations fail to show. From the local value of the shock normal angle, where the grey scale covers the range $\theta_{Bn} = 30°$ (white) to $\theta_{Bn} = 5°$ (black), it is clear from correlating these figures that the change from sharp shock transition to irregular occurs when a region of low instantaneous θ_{Bn} is convected into the field jump. The large-amplitude waves, as they arrive at the shock, force the shock to adjust to the newly changing upstream conditions. This results in a retreating shock ramp (in the average shock frame), and a decay of the sharp profile to a flatter, more extended and irregular transition. This in turn causes a switch-off of the production of backstreaming ions. The arrival of the upstream wave also correlates with the production of backstreaming ions ahead of the main jump in magnetic field amplitude. The correlation between low instantaneous θ_{Bn}, bursty production of backstreaming ions and the transition to an irregular magnetic structure is very good, even down to the mini-reformation cycles.

An apparent prerequisite for reformation to occur is that, in the shock frame, the group velocity of the upstream waves is directed downstream, i.e., the wave energy is transported back into the shock. Krauss-Varban and Omidi (1991) concluded, from hybrid simulations of quasi-parallel shocks with different Mach numbers, that the shock becomes unsteady when the energy flux of waves with downstream directed group velocity exceeds 10 % of the flux given by the upstream background magnetic field and the Alfven velocity Bv_A. Figure 6 shows the dramatic increase in the magnetic energy flux of upstream waves with downstream directed group velocity as a function of Mach number.

However, in order to drastically disturb the shock by changing the upstream condition and to steepen up to a new shock the waves have to grow in amplitude as they are convected into the shock. This is only possible by interaction with existing diffuse ions or with more specularly reflected ions closer to the shock. In a computer experiment a quasi-parallel shock has been followed for some time and a certain reformation cycle was recorded. Figure 7 (Scholer and Burgess 1992) shows in the upper panel a small part of the simulation domain,

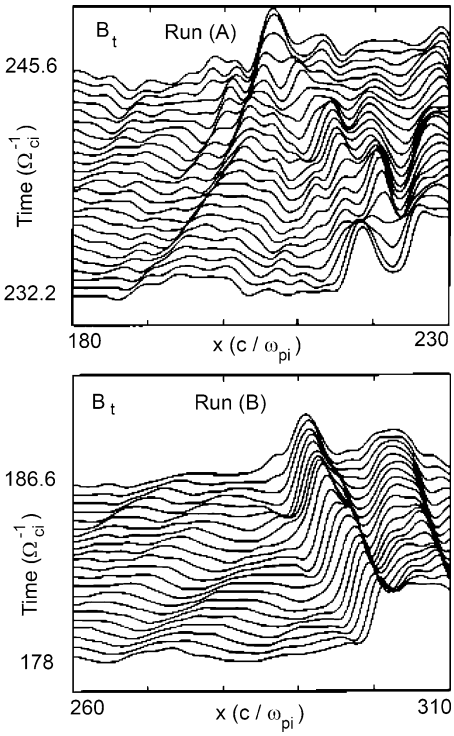

Fig. 7 Time development of the tangential magnetic field for a $\theta_{Bn} = 20°$, $M_A = 4.6$ shock. Results are shown in the simulation frame so that the shock travels to the left. Shown is part of the simulation box and the time evolution near the shock. In the run shown in the *bottom panel* all backstreaming ions have been eliminated within $80c/\omega_{pi}$ upstream of the shock after $t\Omega_c t = 150$. From Scholer and Burgess (1992)

and the approaching wave crest can be followed in time as the wave is convected toward the shock until the upstream edge becomes the reformed shock. The simulation run was repeated and at $\Omega_c t = 150$ (after the upstream wave train was established) all backstreaming ions in a region of 80 c/ω_{pi} upstream from the shock were removed. In particular no subsequent new backstreaming ions were allowed for. In the lower panel it can be seen that while the wave is convected into the shock it does not steepen up to a new shock front.

The mechanisms for the emergence of large amplitude magnetic field pulsations are worth considering in more detail. The consistent observation of large amplitude pulsations near the Earth's quasi-parallel bow shock and their occurrence in simulations have led to a picture of the quasi-parallel shock as being a patchwork of large amplitude pulsations with "inter-pulsation" plasma sandwiched between the pulsations (Schwartz and Burgess 1991). Figure 8 is a schematic of the relation between large amplitude pulsations (shaded ellipses), magnetic field (dashed lines), and bulk flow (double arrows). The pulsations are decelerated in the shock rest frame, which means that their velocity with respect to the plasma rest frame increases, they are deflected and merge as they convect toward what becomes the downstream state.

In 1-D simulations of quasi-parallel shocks with θ_{Bn} exceeding ~20° the low frequency upstream waves steepen up into large amplitude pulsations in a region very close to the shock. An incoming wave interacts with the shock, producing an associated increased density of diffuse and/or nearly specularly reflected ions. Figure 9 (Scholer 1993) shows for a shock with $\theta_{Bn} = 30°$, $M_A = 4.6$ the ion phase space density, the log of the backstreaming ion density (the solar wind density is normalized to 1), and the two magnetic field components B_z, B_y versus x within a region of $100c/\omega_{pi}$ around the shock (at ~$420c/\omega_{pi}$. As can be seen from the phase space plot there are no specularly reflected ions upstream of the

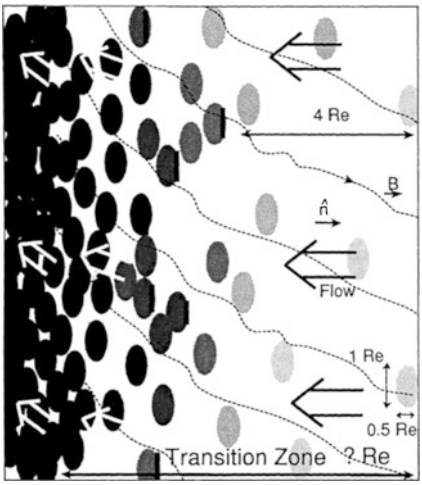

Fig. 8 Schematic of the relation between large amplitude pulsations (*shaded ellipses*), magnetic field (*dashed lines*), and bulk flow (*double arrows*). From Schwartz and Burgess (1991)

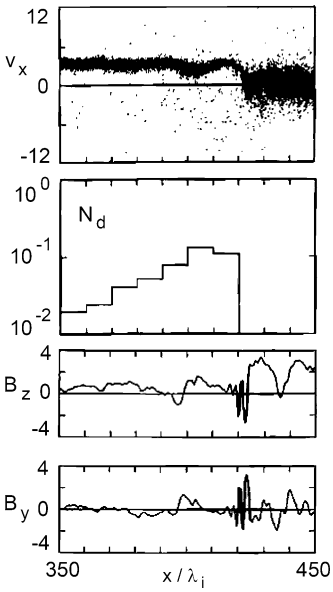

Fig. 9 Ion phase space, the number of backstreaming ions normalized to the far upstream ion density, B_z and B_y versus x normalized to the ion inertial length at one particular time during a 1-D hybrid simulation of a $\theta_{Bn} = 30°$, $M_A = 4.6$ shock. From Scholer (1993)

shock during this time; however, close to the shock the density of diffuse ions drastically increases and exceeds a value of 13 % of the far upstream ion density. This demonstrates that the growth of the shocklet with the upstream steepened edge near $x \sim 400c/\omega_{pi}$ is apparently due to interaction with the increasing number density of diffuse ions. Although this result may depend to some extent on how ions are counted as "diffuse." Attached to the shock ramp is a whistler wave which is due to dispersion during steepening of the shock ramp. In the steepened portion of the wave the upstream ions' bulk velocity decreases, indicating that steepening is in part also due to energy loss of the solar wind. As the large positive B_y of the shocklet reaches the shock ramp a cloud of ions is specularly reflected. However, the specularly reflected ions are trapped within the approaching pulsation which results in a further increase of the pulsation amplitude.

One dimensional simulations constrain the wave vectors to the aligned with the shock normal, but simulations in more than one spatial dimension result in upstream waves with wave vectors mainly in the magnetic field direction, in agreement with the expectations of linear theory for beam instabilities. In 2-D hybrid quasi-parallel shock simulations it has been seen that field-aligned low frequency waves evolve to have their wave vector direction closer to the shock normal direction once they have steepened up into shocklets or pulsations (Scholer et al. 1993). This can be explained by refraction of the waves/pulsations in the region of increasing diffuse ion density: as can be seen from Fig. 4 the velocity of the steepening pulses decreases in the shock frame as the pulse is convected toward the shock, i.e., the upstream directed velocity in the upstream plasma rest frame increases as the pulse approaches the shock. Let us assume that to zeroth order the pulses obey Snell's law as they are amplified in the region of increasing diffuse ion density close to the shock transition. Let us also assume that an upstream boundary parallel to the shock front separates a region of rather low diffuse ion density from a region of high diffuse ion density where the phase velocity of the waves/pulsations in the upstream rest frame is almost equal to the shock Mach number. Snell's law requires conservation of the shock frame wave frequency and tangential wave length at the boundary. This is only possible when the wavelength in the region of decreasing phase velocity in the shock frame ion also decreases. In order to keep the wavelength parallel to the boundary constant, the waves have to be refracted away from the magnetic field direction towards the boundary normal direction. Thus as the phase velocity in the shock frame decreases the wave fronts become more aligned with the shock front. Some observational evidence for this effect is presented in Lucek et al. (2008).

Simulations have also given evidence that pulsations, and subsequent associated reformation, can also be induced by specularly reflected ions. Hybrid shock simulations have been performed where the diffuse upstream ions have been removed from the system a distance $50c/\omega_{pi}$ upstream of the shock position in order to suppress the long wavelength upstream waves (Thomas et al. 1990). These artificial shocks nevertheless exhibit an unsteady behavior and are reforming. One mechanism for the unsteadiness is the periodically occurring bursts of specularly reflected ions which propagate upstream and interact with the incoming solar wind to produce large amplitude pulsations which are almost standing with respect to the shock. The shock retreats and these pulsations become the new reformed shock ramp. Figure 10 shows results from a $\theta_{Bn} = 30°$, $M_A = 6$ shock simulation where upstream waves have largely been suppressed. Shown is the magnetic field magnitude, the B_y component, the ion density, and ion phase space versus x for two different times which are $6\Omega_c^{-1}$ apart. Note that the range in x has been shifted by $5.5c/\omega_{pi}$ to the left between the left hand plot and the right hand plot. At $t = t_0$ a cold beam of specularly reflected ions (negative v_x) can be seen to emerge from the shock. This beam has strongly interacted $6\Omega_c^{-1}$ later with the incident ion beam: at the upstream edge the two have coupled and peaks in ion density n_i and magnetic field B build up at the upstream edge. The upstream edge has essentially taken over the role of the reformed shock ramp. The new downstream region is not uniform, i.e., the cool and hot parts of the incident and reflected ion beam plasmas have not yet completely phase mixed. This situation is rather similar to the two state temperature often found downstream of the ramp of Earth's bow shock (Thomsen et al. 1990b). This is suggestive that at a collisionless shock reformation can actually be induced by specularly reflected ions without any interaction with upstream waves. However, it has to be kept in mind that the simulations which show this involve the removal of foreshock ions, and therefore the generation of associated waves, which are an intrinsic part of the quasi-parallel shock.

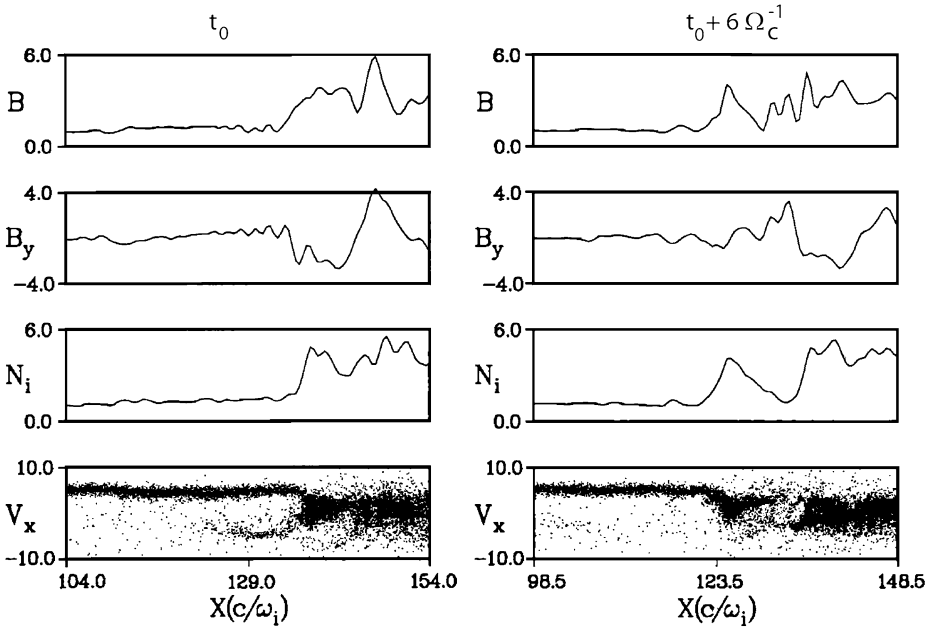

Fig. 10 Profiles of $|B|$, B_y, n_i, $v_x - x$ phase space versus x for a limited range of x around a simulated $\theta_{Bn} = 30°$, $M_A = 6$ shock where upstream diffuse ions have been removed in order to largely suppress low frequency upstream waves. From Thomas et al. (1990)

Let us now focus in more detail on the incident ion-reflected ion beam interaction. The interaction of a spatially limited beam of cold ions with an incident cold ion beam has been the topic of considerable research. In the parallel limit, i.e., magnetic field parallel to the incident beam and a spatially limited beam flowing in the opposite direction, the interaction involves the excitation of ion/ion beam instabilities. For the high reflected beam densities of over 10–20 % it is expected that the nonresonant (firehose type) right hand beam instability has the largest growth rate. However, as shown by Onsager et al. (1991a) two important facts modify the interaction compared to the homogeneous plasma case: Firstly, the time a growing wave spends in contact with the finite length beam is important for its final amplitude. The large group velocity (relative to the beam) of the nonresonant mode therefore limits their growth. The resonant mode has a smaller growth rate; however the smaller group velocity allows the waves to interact longer with the reflected ions, so that they can grow to larger amplitudes. Secondly, the beam progressively spreads in space due to velocity dispersion. This leads to a cold, high velocity, low density beam, ahead of the main beam population, in which the resonant beam instability has a larger growth rate compared to the nonresonant instability. The coupling of incident beam and reflected beam leads to a transfer of the beam velocity difference into thermal energy. For a beam density ∼40 % and a beam length of the order of $100c/\omega_{pi}$, it turns out from the simulations that 50 % of the relative velocity can be transferred into thermal energy within 5 ion gyro-times. However, the discussion of the interaction of a finite length beam with an incident beam in the limit of field-parallel propagation is largely academic. The magnetic field upstream of a shock is either inclined relative to the incident (and specular reflected) bulk flow due to a finite θ_{Bn} and/or the angle of the magnetic field relative to the velocity of the reflected ions is considerably modified due to the surrounding wave field.

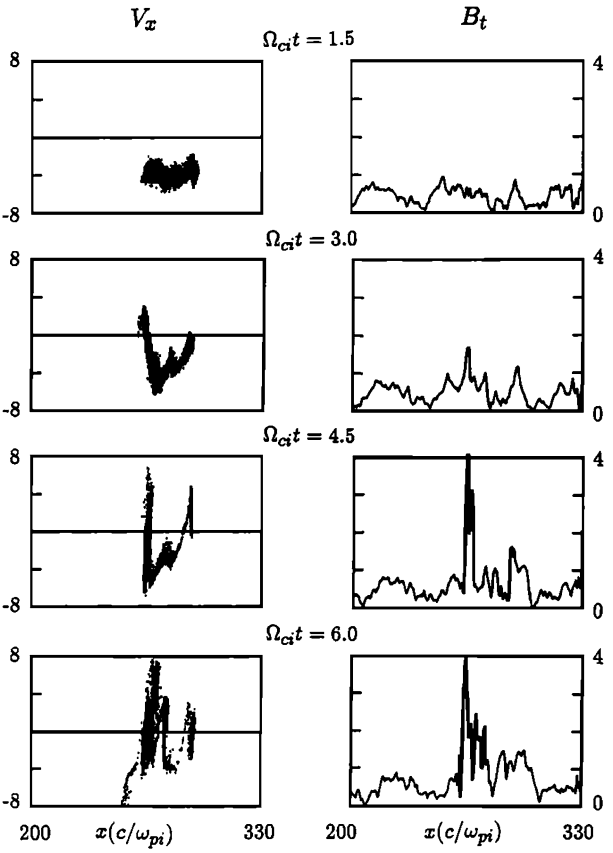

Fig. 11 $v_x - x$ phase space plots of (*left*) a finite length beam placed into an upstream low frequency wave field and (*right*) tangential magnetic field B_t at various times after the beam has been placed into the upstream region. From Scholer and Burgess (1992)

When treating the reflected particles as test particles in a uniform upstream flow, the distance they reach upstream can be found from their motion in the upstream magnetic field and $\mathbf{V}_u \times \mathbf{B}$ motional electric field (Onsager et al. 1991b). For $\theta_{Bn} > 30°$ the distance d normal to the shock where the normal component of velocity is zero is given by

$$d = M_A\left[\Omega_c\tau\left(2\cos^2\theta_{Bn} - 1\right) + 2\sin^2\theta_{Bn}\sin\Omega_c\tau\right]c/\omega_{pi}, \tag{1}$$

where the distance d is reached at the time τ given by

$$\Omega_c\tau = \arccos\left[\frac{1 - 2\cos^2\theta_{Bn}}{2\sin^2\theta_{Bn}}\right]. \tag{2}$$

For $M_A = 5$ and $\theta_{Bn} = 30°$ specularly reflected test particles reach zero normal velocity by $\Omega_c\tau = \pi$ and at $d \approx 8c/\omega_{pi}$. It has been suggested that the reflected ions will then accumulate and may considerably affect the upstream density, flow velocity, and magnetic field. An example of the ensuing interaction is shown in Fig. 11 (Scholer and Burgess 1992). A 1-D hybrid simulation of a $\theta_{Bn} = 20°$, $M_A = 4.6$ shock was run up to some time, at which point the region upstream of the shock was extracted and placed into a new system with open boundaries together with a finite length beam representing cold specularly reflected ions. The beam length is assumed to be $30c/\omega_{pi}$ and the beam density is 40 % of the upstream ion density. The upper two panels of Fig. 11 show the $v_x - x$ phase space of the beam ions and the magnitude of the magnetic field tangential to the shock B_t shortly after the beam has

been placed into the simulation. Due to the large local θ_{Bn} in the upstream waves evident in the top right hand panel the beam ions immediately begin to interact with the incident ion population. At the upstream edge the beam ions are decelerated and deflected parallel to the shock plane. This leads to a local increase in beam density and in turn to a compression of the tangential magnetic field. The stronger field inhomogeneity results in a positive feedback loop generating the large magnetic field perturbation. At the same time the incident beam is decelerated at the upstream edge of the pulsation; the energy for the large amplitude pulsation comes in part from energy transfer of the bulk velocity of the incident ions. The positive feedback process between reflected ion deflection and magnetic field steepening produces the reformation seen in Fig. 11. Although this process may also work without upstream low frequency waves, it is however facilitated as a low frequency wave approaches the shock, thereby producing an increased tangential magnetic field component, and thus a larger local θ_{Bn}.

With a few exceptions, such as the work of Pantellini et al. (1992), the majority of early simulation studies of the quasi-parallel shock used the hybrid simulation technique, since it was not possible to carry out full particle (PIC) simulations with an extended upstream region; to follow the shock over ion gyration time scales; and to use a reasonably large ion to electron mass ratio. Pantellini et al. (1992) used an implicit PIC code, with, because of computational constraints, an unrealistic value of $m_i/m_e = 100$. With ever increasing computer capability, large-scale PIC simulations have become possible. Such PIC simulations are desirable in order to study the influence of whistler waves, either phase standing with the shock or attached to the upstream edge of steepening shocklets. These waves, with wavelengths less than an ion inertial length, cannot be properly resolved by hybrid simulations and their damping rate cannot be modelled correctly. Some early hybrid simulations have actually suggested that the dispersive whistler waves provide the required dissipation at the quasi-parallel shock (Kan and Swift 1983).

Results from a 1-D PIC simulation of a $\theta_{Bn} = 30°$, $M_A = 4.7$ shock with a mass ratio of $m_i/m_e = 100$ and $\omega_{pe}/\Omega_{ce} = \sqrt{10}$ are shown in Fig. 12 (Scholer et al. 2003). The total system size for this simulation is $200c/\omega_{pi}$. The left hand side of Fig. 12 shows from top to bottom B_z, the shock normal potential Φ, the ion bulk speed in the normal direction, and the ion density n_i versus x. Various magnetic field structures are numbered with 1 through 4. The shock transition was shortly before this time at the upstream edge of pulsation 1 and is now at the upstream edge of pulsation 2 as indicated by the sudden drop in bulk speed and by the increase of the ion density. Pulsation 3 has a steepened upstream edge and becomes later the reformed shock. Phase standing whistler waves are attached to the shock ramp (upstream edge of pulsation 2) and a smaller amplitude whistler train is attached to the steepening edge of pulsation 3. The left hand side of Fig. 12 shows the temporal development of pulsation 3 (stacked profiles of the magnetic field B_z) component. Arriving pulsation 3 runs into the whistler train attached to the ramp and the waves are damped, at the same time pulsation 3 steepens and emits a new whistler wave train at the upstream edge. The damping leads to a local heating of the ions in the trailing part of the pulsation. This suggests that dispersive whistlers also play an active role in shock dissipation; however this is due to the interaction with a newly arriving pulsation. During the emergence of a new shock ramp specularly reflected ions are produced; these ions are subsequently scattered in the large amplitude phase standing whistler. This leads to a deviation of the phase space position of specular reflected ions from the nominal one based on θ_{Bn}. But again nothing final can be said about wave amplitudes simply from results of 1-D simulations. Another issue to consider is the role of the artificially low m_i/m_e ratio, and further work is required to investigate to what extent the simulated structure changes as m_i/m_e approaches its real value.

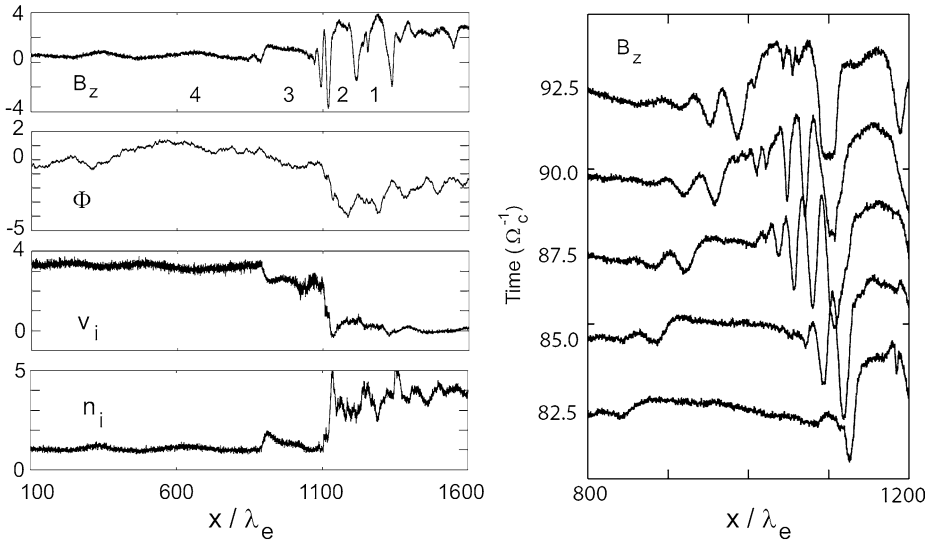

Fig. 12 (*Left*) PIC simulation results for a $\theta_{Bn} = 30°$, $M_A = 4.7$ shock. Magnetic field B_z component, shock normal potential Φ, ion bulk velocity and ion density versus x at one particular time. (*Right*) Time sequence of profiles of B_y; second profile from bottom corresponds to time of overview shown to the left. From Scholer et al. (2003)

The mechanism discussed for shock reformation so far involves the occurrence of large amplitude pulsations which become an integral part of the shock thermalization process. This mechanism involves the production of backstreaming particles, either suprathermal diffuse ions or specular reflected ions. In hybrid simulations of collisionless shocks an experiment can be made where all backstreaming ions are eliminated as soon as they are generated. It has been shown that in such an experiment the shock still reforms. This is due to an instability in a small shock interface region where the incident ion beam and part of the downstream hot ion distribution overlap. Since this instability occurs in a very limited region at the shock interface it has been termed the interface instability (Winske et al. 1990). Linear theory fails to describe such an instability since the region where this instability would be excited is possibly smaller than the wavelength of the (linearly unstable) waves. It is thought that the waves at the interface can rapidly grow to large amplitudes and mimic reformation. Figure 13 shows results from a numerical experiment where initially two beams fill the separate halves of space. The "upstream" beam has a velocity of $M_A = 5$, the downstream beam has twice the temperature of the upstream beam and 2.4 the upstream density and is at rest in the simulation system. The magnetic field is inclined by 5° with the x (simulation) direction. The upper panel of Fig. 13 shows the B_z magnetic field component stacked in time, the bottom panel exhibits the phase angle Φ of the magnetic field defined by $\tan\Phi = B_z/B_y$. One sees that large amplitude waves are generated at the interface (at $x = 200c/\omega_{pi}$, which propagate downstream and are subsequently replaced by new waves. From the increase of phase angle with x (lower panel) it can be concluded that these waves have right hand (positive) helicity.

More direct proof of an instability occurring at the shock interface can be seen from a 1-D hybrid simulation of a higher Mach number, more parallel shock with $M_A = 6$ and $\theta_{Bn} = 10°$ in Krauss-Varban (1995) (Fig. 14). The magnetic field displays a similar behaviour as the shock shown earlier in Fig. 4 (Scholer and Terasawa 1990), in that upstream fast magne-

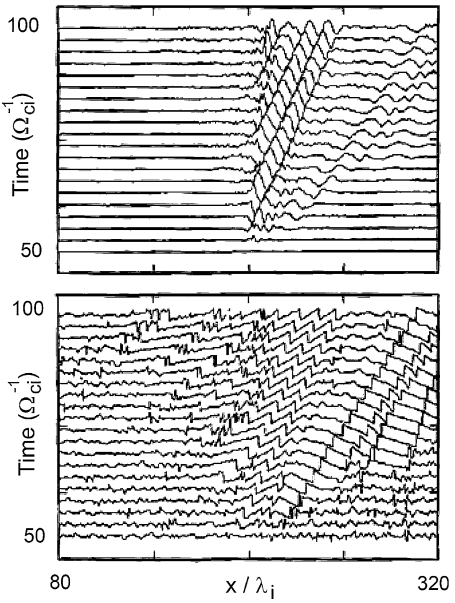

Fig. 13 Time sequence of (*top*) B_z and (*bottom*) phase angle profiles over portion of a 1-D hybrid simulation of a two-stream interaction (upstream parameters $\theta_{Bn} = 5°$, $\beta_i = 1$; downstream parameters $n_2/n_1 = 2.4$, $\beta_i = 2$). From Winske et al. (1990)

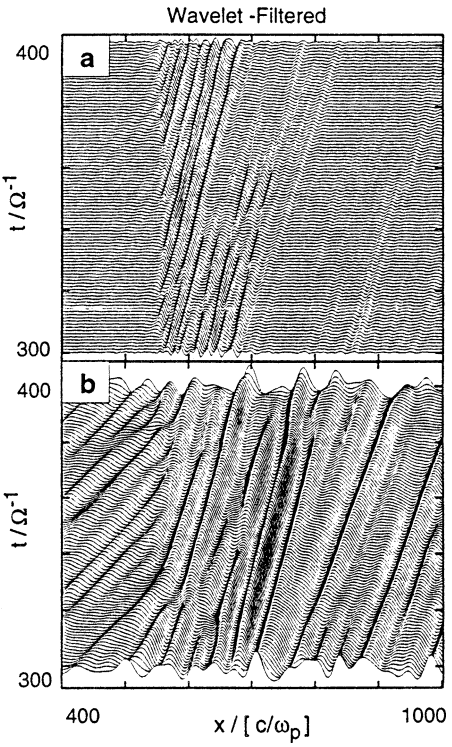

Fig. 14 Stack of wave-filtered B_y in the shock frame. (**a**) Wavelet components 4 and 5 showing the monochromatic waves immediately behind the shock; (**b**) wavelet components 1–3 demonstrating the upstream waves as they mode convert through the shock interface. From Krauss-Varban (1995)

tosonic waves steepen and at times disturb the shock transition. Instead of displaying a stack plot (in time) of the B_y magnetic field component the data has been filtered using a wavelet method. This allows a meaningful interpretation of localized structures and is of particular advantage when the waves consist of only a few cycles and/or have signatures of steepened edges. The upper panel of Fig. 14 shows contributions from high wavelet numbers (4 and 5 from the ${}_{10}\psi$-wavelet system). The lower panel shows the remainder after subtracting out the former. In the upper panel it can be seen that small wavelength rather monochromatic waves are produced right at the shock interface. (Note that the data are plotted in the shock frame so that the shock stays at constant x.) These small wavelength waves are produced at the shock interface and the phases propagate downstream. After a distance $\sim 150 c/\omega_{pi}$ these interface waves are damped out. Conversely, the larger wavelength waves upstream can be seen to undergo a change of their properties at the shock interface and to continue in the whole downstream region. The change at the shock interface is due to the mode conversion of the upstream fast magnetosonic wave into a downstream Alfvén wave. Close inspection of the ion phase space at a particular time at various positions through the shock reveals that ion thermalization occurs in the whole transition region defined by the small wavelength interface waves.

In the medium and higher Mach number range up to $M_A \sim 8$ the interface waves are right hand polarized and their wavelength dependence on θ_{Bn} and M_A agrees with excitation by the ion/ion right hand resonant instability for the local plasma properties at the shock interface (Winske et al. 1990). These monochromatic waves are damped downstream over a distance of 100–200 ion inertial lengths (Krauss-Varban 1995). Beyond this distance downstream from the shock the waves produced upstream and then mode-converted at the shock are the main wave modes. At Mach numbers above $M_A \sim 8$ the resonant as well as the ion/ion right hand nonresonant, firehose type instability gets excited in the interface region (Scholer et al. 1997). This is due to the rapid increase of the growth rate of the nonresonant instability with relative velocity between beam and background plasma. These resonant and nonresonant waves then have very large amplitudes and are the dominant component of the far downstream turbulence.

4 Summary

The quasi-parallel shock operates by a complex interplay between a number of different components: particle injection/reflection; nonlinear wave-particle coupling including coherent structures; energetic particles and foreshock waves. The key to understanding the quasi-parallel shock depends on the microphysics of the extended transition zone from upstream to downstream flow, where all these components interact. A companion review (Burgess et al. 2012) describes particle acceleration mechanisms, and kinetic processes for particle injection, and consequently this review has concentrated on the magnetic structure and behaviour of waves and particles at the shock. However, it is worth emphasizing the point that it may be difficult to separate the processes of diffusive acceleration from the microphysics of the shock. Theories of diffusive acceleration often make assumptions abut wave-particle scattering that have to be tested against the microphysics of the shock transition. And, as it has been shown, the waves of the foreshock are convected into the shock transition, thereby affecting (or even controlling) the microphysics. This poses a puzzle: namely, how does the overall, global system arrange the fine tuning between energetic ion acceleration efficiency, particle injection and foreshock/shock coupling?

It can also be noted that this review has concentrated on the high Mach number shocks seen at the terrestrial bow shock and elsewhere in the heliosphere, but it is possible that new

models of wave-particle-flow coupling within the quasi-parallel shock will be required for the very high Mach number regime as found in some astrophysical systems (e.g., Gargaté and Spitkovsky 2012).

We have discussed the quasi-parallel shock mostly in terms of computer simulations, but from the discussion of underlying concepts there arises another puzzle about the absolute scale of the shock. As a shock simulation continues in time energetic particles spread further and further away from the "nominal" shock position, extending the foreshock. The question arises whether there is any intrinsic scale which limits this process. Some studies (e.g., Giacalone et al. 1993) have used a "free-escape boundary" where upstream energetic particles are removed at some fixed distance, to model a shock with spatial or, equivalently, temporal limitations. Alternatively, Sugiyama (2011) has simulated in 1-D an extremely large system with no free-escape boundary, and found that the characteristic energy in the upstream (i.e., the energy of turn-over from a power-law behaviour) increases with time. How the influence of a very large foreshock impacts the microphysics of the shock transition zone (where most of the thermalization occurs) is still an open question, as is the behaviour when full three-dimensionality is taken into account.

Finally, we consider some the current challenges which have to be addressed in order to achieve progress in understanding the physics of the quasi-parallel shock. Although many of the original concepts of the pulsation shock were rooted in observations, a major part of the overall view of the shock dissipation process is now based on simulations. It has become important to return to modern observations to validate the results from simulations. Of course, many of the observational problems associated with the quasi-parallel shock remain, such as the difficulty of separating temporal and spatial variations. However, problems such as the ion injection mechanism and electron heating are relatively under-explored and would benefit from further observational work.

In terms of physical understanding, possible the greatest challenge of the quasi-parallel shock is its multi-scale nature. The pulsation shock layer is embedded in turbulence between the upstream foreshock and the downstream flow region. How important is the character of the ULF foreshock for the qualitative (and quantitative) behaviour of the pulsation shock layer? At smaller scales, there is yet again competition between scales: At quasi-parallel geometries wave dispersion plays a crucial role, but whistler mode dispersion, as is observed, implies electron scale damping which is not properly modelled in the hybrid simulations which dominate this field. To what extent does pulsation evolution depend on processes which act at scales smaller than can properly be included in the hybrid simulations? On the other hand, does pulsation growth have to be modelled using the large scales which can only (at the present time) be realised by hybrid simulations? These questions may be addressed by larger and more detailed PIC and multi-dimensional simulations. It would also be interesting to extend the simulations by using realistic mass ratio in order to analyse fine scale structure in the shock transition region. However, as one is forced to consider larger and larger scales associated with diffusive particle acceleration and foreshock waves, eventually the type and configuration of the shock driver or obstacle has to be taken into account. Because of the relatively long time scales for diffusive acceleration, and the long length scales for the foreshock, it becomes possible that to understand a particular quasi-parallel shock it might have to be necessary to take into account the totality of its environment, including sources of upstream turbulence, sources of already accelerated energetic particles, the three-dimensional configuration of the interaction, and so on. Within this complex interaction one would then hope to find those properties of the quasi-parallel shock that are universal and can be applied to other astrophysical systems where we do not have the riches of observations available from heliospheric shocks.

Acknowledgements D. Burgess acknowledges support of STFC grant ST/J001546/1.

References

D. Burgess, Cyclical behavior at quasi-parallel collisionless shocks. Geophys. Res. Lett. **16**, 345–349 (1989)
D. Burgess, Foreshock-shock interaction at collisionless quasi-parallel shocks. Adv. Space Res. **15**, 159–169 (1995). doi:10.1016/0273-1177(94)00098-L
D. Burgess, E. Möbius, M. Scholer, Ion acceleration at the Earth's bow shock. Space Sci. Rev. **173**(1–4), 5–47 (2012). doi:10.1007/s11214-012-9901-5
D. Burgess, E.A. Lucek, M. Scholer, S.D. Bale, M.A. Balikhin, A. Balogh, T.S. Horbury, V.V. Krasnoselskikh, H. Kucharek, B. Lembège, E. Möbius, S.J. Schwartz, M.F. Thomsen, S.N. Walker, Quasi-parallel shock structure and processes. Space Sci. Rev. **118**, 205–222 (2005). doi:10.1007/s11214-005-3832-3
J.P. Eastwood, E.A. Lucek, C. Mazelle, K. Meziane, Y. Narita, J. Pickett, R.A. Treumann, The foreshock. Space Sci. Rev. **118**, 41–94 (2005). doi:10.1007/s11214-005-3824-3
L. Gargaté, A. Spitkovsky, Ion acceleration in non-relativistic astrophysical shocks. Astrophys. J. **744**, 67 (2012). doi:10.1088/0004-637X/744/1/67
J. Giacalone, D. Burgess, S.J. Schwartz, D.C. Ellison, Ion injection and acceleration at parallel shocks—Comparisons of self-consistent plasma simulations with existing theories. Astrophys. J. **402**, 550–559 (1993). doi:10.1086/172157
K.I. Golden, L.M. Linson, S.A. Mani, Ion streaming instabilities with application to collisionless shock wave structure. Phys. Fluids **16**, 2319–2325 (1973). doi:10.1063/1.1694299
J.T. Gosling, M.F. Thomsen, S.J. Bame, C.T. Russell, Ion reflection and downstream thermalization at the quasi-parallel bow shock. J. Geophys. Res. **94**, 10027–10037 (1989). doi:10.1029/JA094iA08p10027
E.W. Greenstadt, F.L. Scarf, C.T. Russell, R.E. Holzer, V. Formisano, P.C. Hedgecock, M. Neugebauer, Structure of a quasi-parallel, quasi-laminar bow shock. J. Geophys. Res. **82**, 651–666 (1977). doi:10.1029/JA082i004p00651
J.R. Kan, D.W. Swift, Structure of the quasi-parallel bow shock—Results of numerical simulations. J. Geophys. Res. **88**, 6919–6925 (1983). doi:10.1029/JA088iA09p06919
D. Krauss-Varban, Waves associated with quasi-parallel shocks: Generation, mode conversion and implications. Adv. Space Res. **15**, 271–284 (1995). doi:10.1016/0273-1177(94)00107-C
D. Krauss-Varban, N. Omidi, Structure of medium Mach number quasi-parallel shocks—Upstream and downstream waves. J. Geophys. Res. **961**, 17715 (1991). doi:10.1029/91JA01545
E.A. Lucek, T.S. Horbury, I. Dandouras, H. Rème, Cluster observations of the Earth's quasi-parallel bow shock. J. Geophys. Res. (Space Phys.) **113**, 7 (2008). doi:10.1029/2007JA012756
G. Mann, H. Luehr, W. Baumjohann, Statistical analysis of short large-amplitude magnetic field structures in the vicinity of the quasi-parallel bow shock. J. Geophys. Res. **99**, 13315 (1994). doi:10.1029/94JA00440
T.G. Onsager, D. Winske, M.F. Thomsen, Interaction of a finite-length ion beam with a background plasma—Reflected ions at the quasi-parallel bow shock. J. Geophys. Res. **96**, 1775–1788 (1991a). doi:10.1029/90JA02008
T.G. Onsager, D. Winske, M.F. Thomsen, Ion injection simulations of quasi-parallel shock re-formation. J. Geophys. Res. **962**, 21183 (1991b). doi:10.1029/91JA01986
T.G. Onsager, M.F. Thomsen, J.T. Gosling, S.J. Bame, C.T. Russell, Survey of coherent ion reflection at the quasi-parallel bow shock. J. Geophys. Res. **95**, 2261–2271 (1990). doi:10.1029/JA095iA03p02261
F.G.E. Pantellini, A. Heron, J.C. Adam, A. Mangeney, The role of the whistler precursor during the cyclic reformation of a quasi-parallel shock. J. Geophys. Res. **97**, 1303–1311 (1992). doi:10.1029/91JA02653
E.N. Parker, A quasi-linear model of plasma shock structure in a longitudinal magnetic field. J. Nucl. Energy **2**, 146–153 (1961). doi:10.1088/0368-3281/2/1/323
M. Scholer, Upstream waves, shocklets, short large-amplitude magnetic structures and the cyclic behavior of oblique quasi-parallel collisionless shocks. J. Geophys. Res. **98**, 47–57 (1993). doi:10.1029/92JA01875
M. Scholer, D. Burgess, The role of upstream waves in supercritical quasi-parallel shock re-formation. J. Geophys. Res. **97**, 8319–8326 (1992). doi:10.1029/92JA00312
M. Scholer, T. Terasawa, Ion reflection and dissipation at quasi-parallel collisionless shocks. Geophys. Res. Lett. **17**, 119–122 (1990). doi:10.1029/GL017i002p00119
M. Scholer, M. Fujimoto, H. Kucharek, Two-dimensional simulations of supercritical quasi-parallel shocks: upstream waves, downstream waves, and shock re-formation. J. Geophys. Res. **98**, 18971 (1993). doi:10.1029/93JA01647
M. Scholer, H. Kucharek, V. Jayanti, Waves and turbulence in high Mach number nearly parallel collisionless shocks. J. Geophys. Res. **102**, 9821–9834 (1997). doi:10.1029/97JA00345

M. Scholer, H. Kucharek, I. Shinohara, Short large-amplitude magnetic structures and whistler wave precursors in a full-particle quasi-parallel shock simulation. J. Geophys. Res. (Space Phys.) **108**, 1273 (2003). doi:10.1029/2002JA009820

S.J. Schwartz, D. Burgess, Quasi-parallel shocks—A patchwork of three-dimensional structures. Geophys. Res. Lett. **18**, 373–376 (1991). doi:10.1029/91GL00138

S.J. Schwartz, D. Burgess, W.P. Wilkinson, R.L. Kessel, M. Dunlop, H. Luehr, Observations of short large-amplitude magnetic structures at a quasi-parallel shock. J. Geophys. Res. **97**, 4209–4227 (1992). doi:10.1029/91JA02581

T. Sugiyama, Time sequence of energetic particle spectra in quasiparallel shocks in large simulation systems. Phys. Plasmas **18**(2), 022302 (2011). doi:10.1063/1.3552026

V.A. Thomas, D. Winske, N. Omidi, Re-forming supercritical quasi-parallel shocks. I—One- and two-dimensional simulations. J. Geophys. Res. **951**, 18809–18819 (1990). doi:10.1029/JA095iA11p18809

M.F. Thomsen, J.T. Gosling, S.J. Bame, C.T. Russell, Magnetic pulsations at the quasi-parallel shock. J. Geophys. Res. **95**, 957–966 (1990a). doi:10.1029/JA095iA02p00957

M.F. Thomsen, J.T. Gosling, S.J. Bame, T.G. Onsager, C.T. Russell, Two-state ion heating at quasi-parallel shocks. J. Geophys. Res. **95**, 6363–6374 (1990b). doi:10.1029/JA095iA05p06363

W.P. Wilkinson, A.K. Pardaens, S.J. Schwartz, D. Burgess, H. Luehr, R.L. Kessel, M. Dunlop, C.J. Farrugia, Nonthermal ions and associated magnetic field behavior at a quasi-parallel earth's bow shock. J. Geophys. Res. **98**, 3889–3905 (1993). doi:10.1029/92JA01669

D. Winske, V.A. Thomas, N. Omidi, K.B. Quest, Re-forming supercritical quasi-parallel shocks. II—Mechanism for wave generation and front re-formation. J. Geophys. Res. **95**, 18821–18832 (1990). doi:10.1029/JA095iA11p18821